Desalination and Water Treatment
www.deswater.com
doi: 10.5004/dwt.2019.23664

144 (2019) 211–223
March

Palladium (II)-catalyzed oxidation kinetics of azidothymidine by heptavalent manganese during water treatment: kinetics, mechanism, and degradation

Vijaykumar S. Bhamare*, Raviraj M. Kulkarni

Department of Chemistry, KLS Gogte Institute of Technology (Autonomous), Affiliated Visvesvaraya Technological University, Belagavi 590 008, Karnataka, India, Tel. +9449466448; email: vbhamare37@gmail.com

Received 14 September 2018; Accepted 22 December 2018

ABSTRACT

The pH-dependent apparent second-order rate constants for uncatalyzed and Pd^{2+}-catalyzed reactions show that Pd^{2+}-catalyzed oxidative degradation of azidothymidine (AZT) by heptavalent manganese is faster than uncatalyzed reaction. Pd^{2+}-catalyzed oxidative degradation of AZT by heptavalent manganese significantly depends on the pH. $HMnO_4$ and Pd^{2+} were found very active species in this catalytic oxidative degradation reaction. The effects of different parameters such as dielectric constant, ionic strength, pH, addition of monomer, and catalyst concentration on the rate of reaction were investigated for uncatalyzed and Pd^{2+}-catalyzed reactions. Eight oxidative degraded products of pure AZT were identified using high-resolution mass spectrometry. The rate constants are determined at a selected temperature, and their temperature variation yields the activation parameters. The values of activation parameters were determined for uncatalyzed and Pd^{2+}-catalyzed reactions. The plausible proposed Pd^{2+} catalytic mechanism shows that oxidative degradation reaction progresses through the formation of catalyst-substrate (Pd-AZT) complex which subsequently forms an intermediate compound with permanganic acid and finally breaks into eight oxidative degraded products. The proposed Pd^{2+} catalytic mechanism is found to be in good agreement with the experimental results and discussed in detail.

Keywords: Water treatment; Heptavalent manganese; Azidothymidine; Palladium (II) catalysis; Environmental waters; Degradation; Kinetics; Mechanism; Emerging contaminants

1. Introduction

Pharmaceutical active compounds (PhACs) have been used in large scale over the past decade to control human and animal diseases with an increase in the annual prescriptions from 2.0 to 3.9 billion [1]. PhACs are not discharged properly in the environment and enter in a landfill or wastewater treatment plant [2]. The presence of PhACs in the environmental water is seen as very harmful to human beings and animals [3,4].

Antiretroviral drugs are designed to slow down or stop the growth of viruses which cause infections in humans and animals [5]. The antiretroviral drug azidothymidine (AZT) has been designed to treat acquired immunodeficiency syndrome infection. AZT has molecular formula $C_{10}H_{13}N_5O_4$. Molecular mass of AZT is 267.24 g mol^{-1} [6,7]. The structure of AZT is shown in Fig. S1. The dissociation constant (pK_a) value of AZT is 9.68 [8]. The solubility of AZT in water is 25 mg mL^{-1} at 25°C [9].

Heptavalent manganese has an ability to oxidize the organic matter, and hence, it is used as a disinfectant in the treatment of drinking water [10,11]. As compared with other oxidizing agents (ozone, chlorine, chlorine dioxide), heptavalent manganese is considered a better oxidant due to its low cost, effectiveness over a broad pH scale, and because of forming harmless oxidative degraded by-products [12]. It does not form any chlorinated by-products during the oxidation process. Heptavalent manganese can be used for the pretreatment process to remove odor from water while chlorination can be used for further water treatment process [13,14].

* Corresponding author.

Mn^{7+} is the most powerful oxidation states of manganese in different media as compared with its other oxidation states [15,16]. It gives unpleasant color to the drinking water during the water treatment. Hence, to prevent the chromaticity, the use of catalyst is very much required to accelerate the rate of degradation of AZT with the low concentration of heptavalent manganese.

The d-block elements have been used extensively to accelerate the rate of redox reactions due to their variable oxidation states [17]. Pd^{2+} is generally utilized either as a catalyst or a reductant due to its reduction potential (Pd^{4+}/Pd^{2+}) of 0.532 V in dilute acid. Many investigations used the catalyst Pd^{2+} in the form of palladium (II) chloride [18,19]. Many researchers have investigated the role of Pd^{2+} in catalyzing the redox reactions due to the commercial importance of reactions catalyzed by Pd^{2+} [20]. Pd^{2+} catalytic mechanism of the redox reaction depends upon the nature of the oxidant and the substrate involved in the reaction. Activated complex is formed between AZT and Pd^{2+} before producing the final products [21,22].

There are no reports found in the literature on the investigation of Pd^{2+}-catalyzed oxidative degradation of AZT by heptavalent manganese. Preliminary kinetic results indicated that the redox reaction of AZT with heptavalent manganese in the acidic medium becomes facile in the presence of extremely small concentration of Pd^{2+}. Hence, Pd^{2+} has been chosen as a catalyst for this work [23].The main aim of present investigation is to understand the redox chemistry of heptavalent manganese, Pd^{2+}, and AZT at pH 6.0 to arrive at a possible mechanism.

2. Experiments and materials

2.1. Chemical reagents

Heptavalent manganese (analytical grade) was purchased from MERCK Specialties Pvt. Ltd., Mumbai, India. The stock solution of heptavalent manganese was standardized using analytical grade oxalic acid as per the standard procedure [24]. The uncatalyzed and Pd^{2+}-catalyzed reactions were studied in different pH media (acidic, neutral, or alkaline) using different buffers to preserve a constant pH in reagent water system. The stock solution of AZT was prepared by dissolving requisite amount of it in double-distilled water. The catalyst palladium (II) chloride (analytical grade) was purchased from Johnson Matthey India Pvt. Ltd., Hyderabad, India and used for the preparation of stock solution by dissolving a suitable quantity of catalyst Pd^{2+} in hydrochloric acid of known strength.

2.2. Instruments

A CARY 50 Bio ultraviolet (UV)-vis spectrophotometer (Varian BV, The Netherlands) having temperature controller was used to record decrease in the absorbance of heptavalent manganese. High-resolution mass spectrometer (HR-MS) system (Thermo Scientific Q Exactive, Waltham, United States.) along with a column Thermo Scientific Hypersil Gold C18 (dimension 150 mm × 4.6 mm to 8 μm) was used to analyze the degraded products while Elico pH meter (Model Li 120) was used to record the pH.

2.3. Kinetic measurements

The concentration of the oxidant heptavalent manganese was taken ten times less than the concentration of substrate AZT to study the kinetic outcomes of uncatalyzed and Pd^{2+}-catalyzed oxidative degradation of AZT by heptavalent manganese under pseudo-first-order conditions at uniform temperature of 298 K. In order to preserve constant temperature, all required solutions of suitable concentration were placed in a thermostat for some time. The catalytic oxidative degradation reaction was investigated by mixing all these thermostatted solutions along with suitable quantity of buffer to preserve the constant pH (6.0) and ionic strength (0.02 mol dm^{-3}). The absorbance of untreated heptavalent manganese is measured using UV-vis spectrophotometer at its maximum absorption wavelength (λ_{max} 526 nm) to check the progress of Pd^{2+}-catalyzed reaction. The kinetic data show that there was no significant interference from the other species at λ_{max} = 526 nm [25]. Spectral changes were recorded using A CARY 50 Bio UV-vis spectrophotometer, which indicates that there was a decrease in the concentration of heptavalent manganese during uncatalyzed and Pd^{2+}-catalyzed reactions. These UV-vis spectral changes of uncatalyzed oxidative degradation of AZT by heptavalent manganese are reported in our recent investigation [26]. The application of Beer's law to heptavalent manganese was verified. The extinction coefficient (ε) was found to be 2281 ± 20 dm^3 mol^{-1} cm^{-1}, which is close to the literature value of ε at 298 K [27]. The graph of log (absorbance) vs. time (min) was plotted by using kinetic data as presented in Fig. S2. The pseudo-first-order rate constants for uncatalyzed (k_U) and catalyzed (k_C) reactions were determined from log (absorbance) vs. time (min) plots. The values of k_U were found very close. Similarly, k_C values were also found very close. This indicates that the order for heptavalent manganese is unity. Further variation in the concentration of heptavalent manganese did not show any considerable change in the values of pseudo-first-order rate constants for uncatalyzed and Pd^{2+}-catalyzed reactions. This proves that the order is unity with respect to heptavalent manganese. The influence of dissolved oxygen on Pd^{2+}-catalyzed oxidative degradation of AZT by heptavalent manganese at environmentally relevant pH was investigated by performing the reaction in air and then in an inert atmosphere of nitrogen. The experimental results show that there is no considerable change in the values of rate constants for uncatalyzed and Pd^{2+}-catalyzed reactions in the presence of N_2 and O_2.

2.4. Product identification

A suitable amount of AZT was added to phosphate buffer (0.02 mol dm^{-3}) of pH 6.0 to obtain an initial concentration of 400 mg dm^{-3}. Heptavalent manganese solution was then added in this mixture to initiate the reaction with a molar ratio 4:1 (heptavalent manganese:AZT). This reaction mixture was placed for 24 h to degrade the AZT completely into different by-products by an oxidant. The small fraction of this reaction mixture was taken out to perform an analysis, and identification of the various by-products formed during the degradation of AZT by heptavalent manganese at environmentally relevant pH using HR-MS system was done. Instrumental conditions such as flow rate (500 μL min^{-1}),

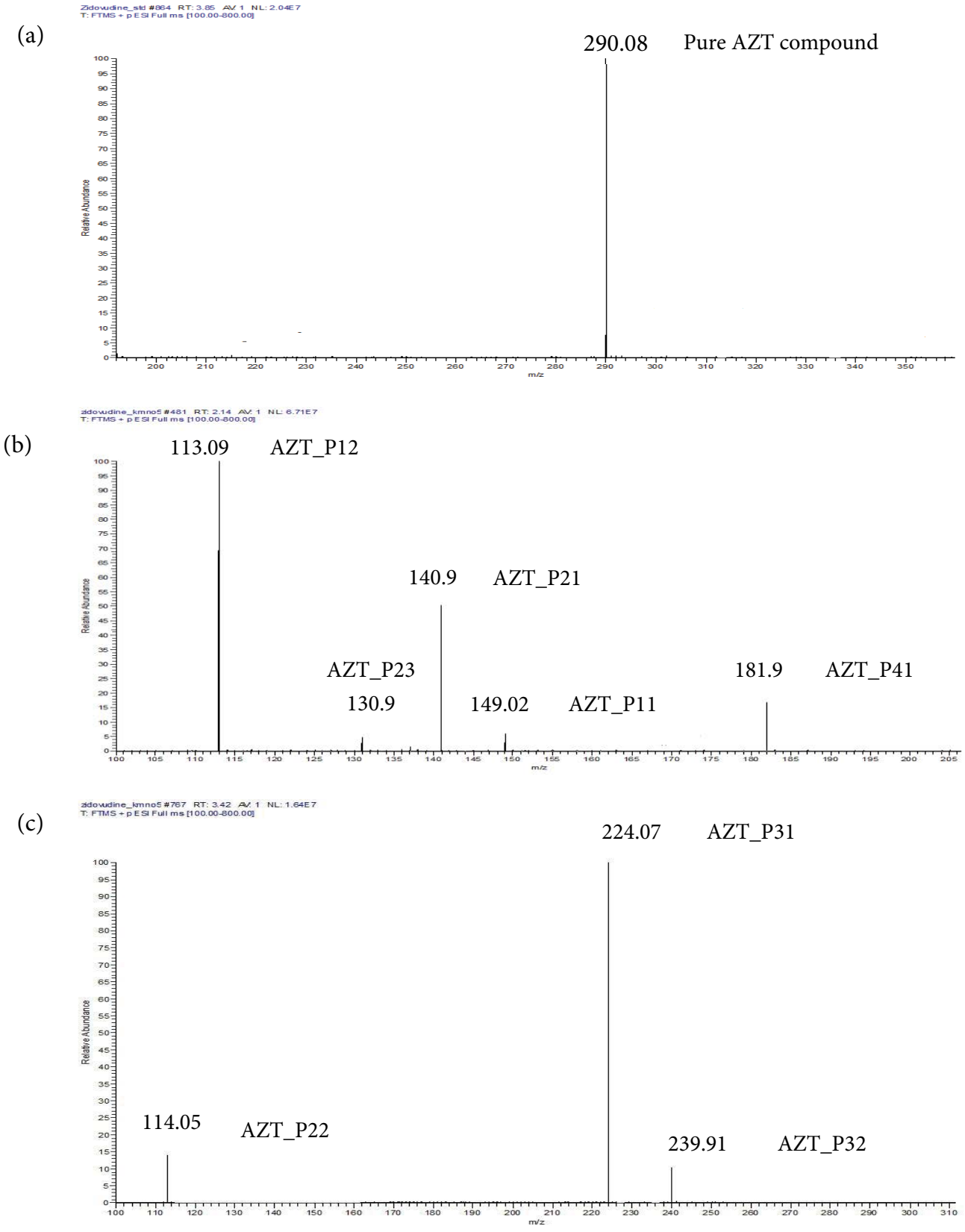

Fig. 1. HR-MS spectra of samples with molecular ion peaks: (a) pure AZT compound, (b) five oxidative degraded products of AZT (AZT_P12, AZT_P23, AZT_P21, AZT_P11, and AZT_P41), and (c) three oxidative degraded products AZT (AZT_P22, AZT_P31, and AZT_P32) by heptavalent manganese at environmentally relevant pH.

pressure (33.2 bar), and mobile phase (acetonitrile:water ratio 50:50) were set up properly. Positive mode electro spray ionization over the mass scan range of 100–800 m/z was used. HR-MS instrumental data provide observed molecular ion peaks for the pure AZT and its degraded product AZT as shown in Figs. 1(a)–(c). Eight degraded products were formed and identified during the oxidative degradation of pure AZT by heptavalent manganese. These products of pure AZT are listed in Table 1.

3. Results and discussion

3.1. Reaction orders

Heptavalent manganese oxidizes AZT at lower pH with a measurable rate in the absence of the catalyst Pd^{2+}. The catalytic oxidative degradation of AZT by heptavalent manganese at lower pH in the presence of catalyst Pd^{2+} takes place in parallel paths. The overall velocity constant (k_O) shows the contributions from velocity constant of uncatalyzed reaction (k_U) and Pd^{2+}-catalyzed reactions. The overall velocity constant (k_O) can also be written as

$$k_O = k_U + k_C \quad (1)$$

$$k_C = k_O - k_U \quad (2)$$

The graphs of log k_{obs} vs. log (concentration) were plotted by changing the concentrations of heptavalent manganese, AZT, catalyst Pd^{2+}, and H^+ ion in each while maintaining other reaction conditions fixed for uncatalyzed and Pd^{2+}-catalyzed reactions to find out the order with respect to [heptavalent manganese], [AZT], [Pd^{2+}], and [H^+]. The concentration of AZT was varied in the range of 5.0×10^{-4} mol dm^{-3} to 3.0×10^{-3} mol dm^{-3} while keeping other experimental conditions fixed. The rate constants (k_U and k_C) were found to be increased with increase in [AZT] in uncatalyzed and Pd^{2+}-catalyzed reactions. Using the values of rate constants (k_U and k_C), the graphs of log k_{obs} vs. log [AZT] were plotted for uncatalyzed and Pd^{2+}-catalyzed reactions. The slopes of straight line plots show that the order with respect to [AZT] is found to be fractional for uncatalyzed and Pd^{2+}-catalyzed reactions as shown in Fig. 2. [Pd^{2+}] was changed from 1.0×10^{-8} mol dm^{-3} to 1.0×10^{-7} mol dm^{-3}

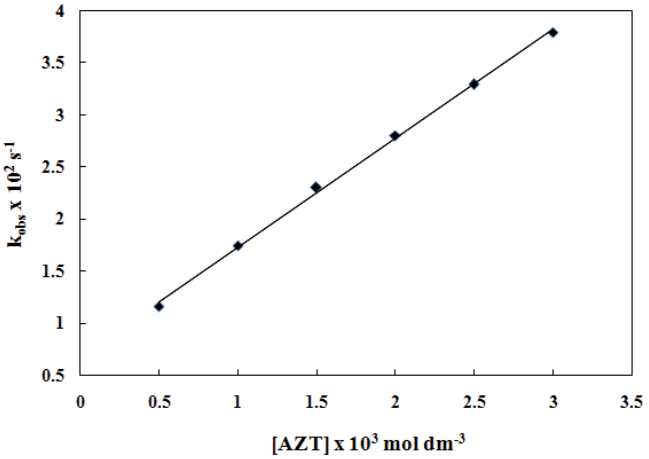

Fig. 2. Influence of variation in [AZT] on Pd^{2+}-catalyzed oxidative degradation of AZT by oxidant heptavalent manganese in acidic medium at pH 6.0 and temperature 298 K. [AZT] = 5×10^{-4} to 3×10^{-3} mol dm^{-3}, [Mn^{7+}] = 1×10^{-4} mol dm^{-3}, [Pd^{2+}] = 5×10^{-8} mol dm^{-3}, [Buffer] = 6×10^{-3} mol dm^{-3}, and Ionic strength (I) = 0.02 mol dm^{-3}.

Table 1
Identified degraded products of AZT during the Pd^{2+}-catalyzed oxidative degradation of AZT by heptavalent manganese at pH 6.0 and temperature 298 K by HR-MS analysis

AZT products	*$t_{R\,(min)}$	M + H^+/M + Na^+ measured	Theoretical mass (Da)	Molecular formula	Difference in measured and theoretical mass	Name of the identified compounds
AZT_P11	3.42	149.02	126.11	$C_5H_6N_2O_2$	–0.08	5-Methyl-1H-pyrimidine-2,4-dione
AZT_P21	2.14	140.90	141.13	$C_5H_7N_3O_2$	–0.23	(3-Azido-2,3-dihydro-furan-2-yl)-methanol
AZT_P12	2.14	113.09	113.11	$C_5H_7NO_2$	–0.02	*N*-(2-Methyl-3-oxo-propenyl)-formamide
AZT_P22	2.14	114.05	115.13	$C_5H_9NO_2$	–1.08	(3-Amino-2,3-dihydro-furan-2-yl)-methanol
AZT_P23	2.14	130.90	131.13	$C_5H_9NO_3$	–0.23	(3-Hydroxyamino-2,3-dihydro-furan-2-yl)-methanol
AZT_P31	3.42	224.07	224.21	$C_{10}H_{12}N_2O_4$	–0.14	1-(5-Hydroxymethyl-2,5-dihydro-furan-2-yl)-5-methyl-1H-pyrimidine-2,4-dione
AZT_P32	3.42	239.91	238.20	$C_{10}H_{10}N_2O_5$	+1.71	5-(5-Methyl-2,4-dioxo-3,4-dihydro-2H-pyrimidin-1-yl)-2,5-dihydro-furan-2-carboxylic acid
AZT_P41	2.14	181.96	181.10	$C_5H_6N_2O_4$	+0.86	3-Hydroxy-5-hydroxymethyl-1H-pyrimidine-2,4-dione

*$t_{R\,(min)}$ indicates retention time in minutes.

while maintaining other experimental reaction conditions constant. The rate of the reaction is faster in the presence of catalyst Pd^{2+} than uncatalyzed reaction. The nature of the plot of log k_C vs. log [Pd^{2+}] is found to be in a straight line, and a slope of the plot shows that the order with respect to catalyst Pd^{2+} is unity. The effect of catalyst clearly indicates that Pd^{2+} is a substantial and potent catalyst for the oxidative degradation of AZT by heptavalent manganese at acidic pH (6.0).

3.2. Influence of variation in ionic strength on reaction rates

This effect was studied for uncatalyzed and Pd^{2+}-catalyzed reactions by varying [Buffer] of pH 6.0 from 0.002 to 0.012 mol dm^{-3} while maintaining other experimental reaction conditions constant. The experimental results show that there is no considerable change in the values of rate constants for uncatalyzed and Pd^{2+}-catalyzed reactions. Hence, the insignificant effect of variation in ionic strength (I) indicates there is no reaction took place between the solvent and heptavalent manganese during the uncatalyzed and Pd^{2+}-catalyzed reactions [28].

3.3. Influence of variation in dielectric constant on oxidative degradation reaction

In order to study the dependence of rate on dielectric constant, the volume of tertiary butanol was varied for uncatalyzed and Pd^{2+}-catalyzed reactions while maintaining other experimental reaction conditions fixed. It was observed from the experimental results that as the dielectric constant decreases, the values of rate constants also decrease for uncatalyzed and Pd^{2+}-catalyzed reactions. The plots of log k_{obs} vs. 1/D were found linear with negative slope as shown in Figs. 3(a) and (b) for uncatalyzed and Pd^{2+}-catalyzed reactions, respectively [10,29].

3.4. Test for the involvement of free radical in oxidative degradation reaction

A suitable quantity of acrylonitrile monomer was mixed with reaction mixtures in acidic medium (pH 6.0) for uncatalyzed and catalyzed reactions to investigate the possibility of the formation of free radicals. Both reaction mixtures were placed for a period of 10 h. Both these reaction mixtures are then diluted with methyl alcohol. There was no formation of any insoluble precipitate in uncatalyzed and Pd^{2+}-catalyzed reactions. This polymerization study confirms that there is no intervention of free radical in catalytic and noncatalytic reactions [30].

3.5. Influence of variation in pH on oxidative degradation reaction

In order to study the influence of pH on the values of rate constants of uncatalyzed and Pd^{2+}-catalyzed reactions, pH was varied from 3.0 to 9.0 using acetate (0.02 mol dm^{-3}), phosphate 0.02 mol dm^{-3}), and borate (0.02 mol dm^{-3}) buffers to preserve a particular pH while maintaining other experimental reaction conditions fixed. It was observed that the values of rate constants (k_U and k_C) are higher in acidic medium than alkaline medium in uncatalyzed and Pd^{2+}-catalyzed reactions. By using values of first-order rate constants at different pH, the graphs of log k_{obs} vs. [AZT] at different pH values (3.0–9.0) were plotted to obtain the second-order rate constants. The values of pH-dependent second-order constants for uncatalyzed reaction (k''_U), catalyzed reaction (k''_C), and overall reaction (k''_O) are listed in Table 2. By using k''_U, k''_C, and k''_O values, the graphs of pH-dependent apparent second-order rate constants (k''_{app}) vs. pH were plotted (Fig. 4).

3.6. Catalytic activity of Pd^{2+}

Moelwyn–Hughes [31] pointed out that the catalytic and noncatalytic reactions take place at the same time in the presence of catalyst. Hence, the overall rate constant (k_O) in the presence of catalyst is mathematically expressed as follows:

$$k_O = k_U + k_C^* \left[Pd^{2+} \right]^y \quad (3)$$

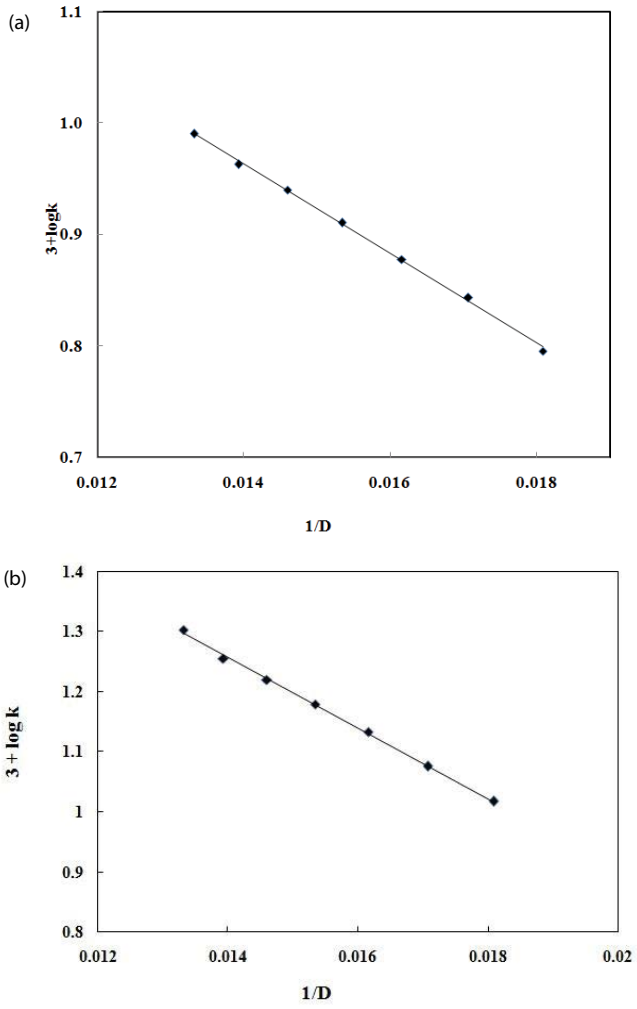

Fig. 3. Influence of variation in dielectric constant on the oxidative degradation of AZT by heptavalent manganese at pH 6.0 and temperature 298 K: (a) uncatalyzed and (b) Pd^{2+}-catalyzed reactions. [AZT] = 1 × 10^{-3} mol dm^{-3}, [Mn^{7+}] = 1 × 10^{-4} mol dm^{-3}, [Pd^{2+}] = 5 × 10^{-8} mol dm^{-3}, [Buffer] = 6 × 10^{-3} mol dm^{-3}, and ionic strength (I) = 0.02 mol dm^{-3}.

Table 2
pH-dependent second-order-rate constant of the effect of variation in pH on the uncatalyzed and Pd^{2+}-catalyzed oxidative degradation of AZT by heptavalent manganese at different pH from 3.0 to 9.0 (temperature 298 K). $[Mn^{7+}] = 1 \times 10^{-4}$ mol dm^{-3}, [AZT] = 1×10^{-3} mol dm^{-3}, $[Pd^{2+}] = 5 \times 10^{-8}$ mol dm^{-3}, [Buffer] = 6×10^{-3} mol dm^{-3}, and ionic strength (I) = 0.02 mol dm^{-3}

pH	k''_U	k''_O	k''_U
3.0	6.11	43.06	36.95
4.0	5.40	37.08	32.40
5.0	4.59	32.27	27.68
6.0	3.65	25.60	21.95
7.0	2.79	19.77	16.98
8.0	1.85	13.10	11.25
9.0	1.11	7.17	6.06

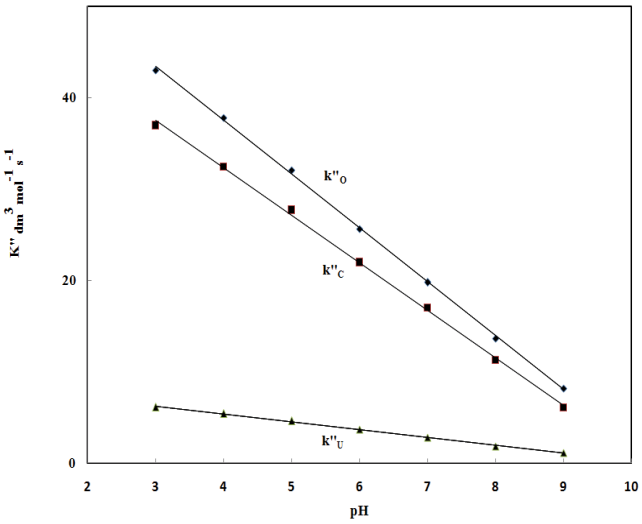

Fig. 4. pH-dependent second-order-rate constants for Pd^{2+} oxidative degradation of AZT by heptavalent manganese at different pH from 3.0 to 9.0 and temperature 298 K. $[Mn^{7+}] = 1 \times 10^{-4}$ mol dm^{-3}, [AZT] = 1×10^{-3} mol dm^{-3}, $[Pd^{2+}] = 5 \times 10^{-8}$ mol dm^{-3}, [Buffer] = 6×10^{-3} mol dm^{-3}, and ionic strength (I) = 0.02 mol dm^{-3}.

In Eq. (3), k_U is observed pseudo-first-order rate constant in the absence of catalyst, K_C^* is the catalytic constant in the presence of catalyst (Pd^{2+}), and 'y' is the order for the catalyst (Pd^{2+}). The experimental value of K_C^* is determined using the following equation:

$$K_C^* = \frac{\left[k_O - k_U\right]}{\left[Pd^{2+}\right]^y} = \frac{k_C}{\left[Pd^{2+}\right]^y} \quad (4)$$

The value of the term 'y' is found unity from the straight line plot of log k_C vs. log $[Pd^{2+}]$ (Fig. S3).

$$K_C^* = \frac{\left(4.39 \times 10^{-2}\right)}{\left(5 \times 10^{-8}\right)} = 8.78 \times 10^5$$

The above Eq. (4) can be rearranged as

$$k_C = K_C^* \times \left[Pd^{2+}\right]^y \quad (5)$$

The above Eq. (5) after taking logarithm becomes

$$\ln k_C = \ln K_C^* + y \ln\left[Pd^{2+}\right] \quad (6)$$

K_c^* can also be obtained from the value of intercept of plot of log k_C vs. log $[Pd^{2+}]$. The rate of Pd^{2+}-catalyzed oxidation of AZT by heptavalent manganese in acidic medium can be written using the experimental values of orders with respect to [AZT], $[Mn^{7+}]$, $[Pd^{2+}]$, and $[H^+]$ as follows:

$$\text{Rate} = \frac{-d\left[MnO_4^-\right]}{dt} = k_U + k_C^*\left[Pd^{2+}\right]^1\left[Mn^{7+}\right]^1\left[AZT\right]^{0.88}\left[H^+\right]^{0.3} \quad (7)$$

3.7. Influence of variation in temperature on oxidative degradation reaction

The kinetics of uncatalyzed and Pd^{2+}-catalyzed reactions were investigated at four different temperatures 283, 288, 293, and 298 K by varying [AZT] from 5×10^{-4} mol dm^{-3} to 3.0×10^{-3} mol dm^{-3} under pH 6.0 while keeping other experimental conditions fixed. Kinetic results of uncatalyzed and Pd^{2+}-catalyzed reactions at 4 different temperatures (283, 288, 293, and 298 K) show that the values of rate constants increase with increase in temperatures. These values of rate constants k (s^{-1}) of the slow step of Scheme 1 are $1.93 \pm 0.12 \times 10^{-2}$, $2.85 \pm 0.16 \times 10^{-2}$, $3.72 \pm 0.19 \times 10^{-2}$, and $4.93 \pm 0.22 \times 10^{-2}$ s^{-1} at 4 different temperatures 283, 288, 293, and 298 K, respectively. These values of k (s^{-1}) were used to determine different activation parameters (E_a, $\Delta H^{\neq}$, $\Delta G^{\neq}$, and $\Delta S^{\neq}$) with the help of Arrhenius plots log k vs. $1/T$ for uncatalyzed (Fig. S4) and Pd^{2+}-catalyzed (Fig. S5) reactions in acidic medium.

The kinetic experimental results show that the values of rate constants are higher at the lower pH values and are lower at the higher pH values. The values of rate constants are higher at lower pH values due to increase in the oxidation potential of heptavalent manganese in higher acidic medium. The values of rate constants are lower at the higher pH (alkaline condition) due to decrease in the oxidation potential of heptavalent manganese. These results indicate that $HMnO_4$ is a dominant species in acidic medium. The rate of formation of $HMnO_4$ is higher at lower pH due to higher concentration of H^+ ions present in the acidic medium. The effect of variation in pH on oxidative degradation reaction indicates that the order with respect to H^+ ion is less than unity (0.3) which confirms the formation of permanganic acid during the reaction in acidic medium. $HMnO_4$ is considered as the strongest species of heptavalent manganese in earlier investigations [32]. Initially, the values of rate constants increase as the pH decreases from alkaline medium to acidic medium of reaction mixture, and then the values of rate constants were attaining a limiting value at very low pH. This confirms the process of protonation is completed and indicates that an active species $HMnO_4$ is only protonated species present in the reaction mixture in acidic medium. It was observed from the

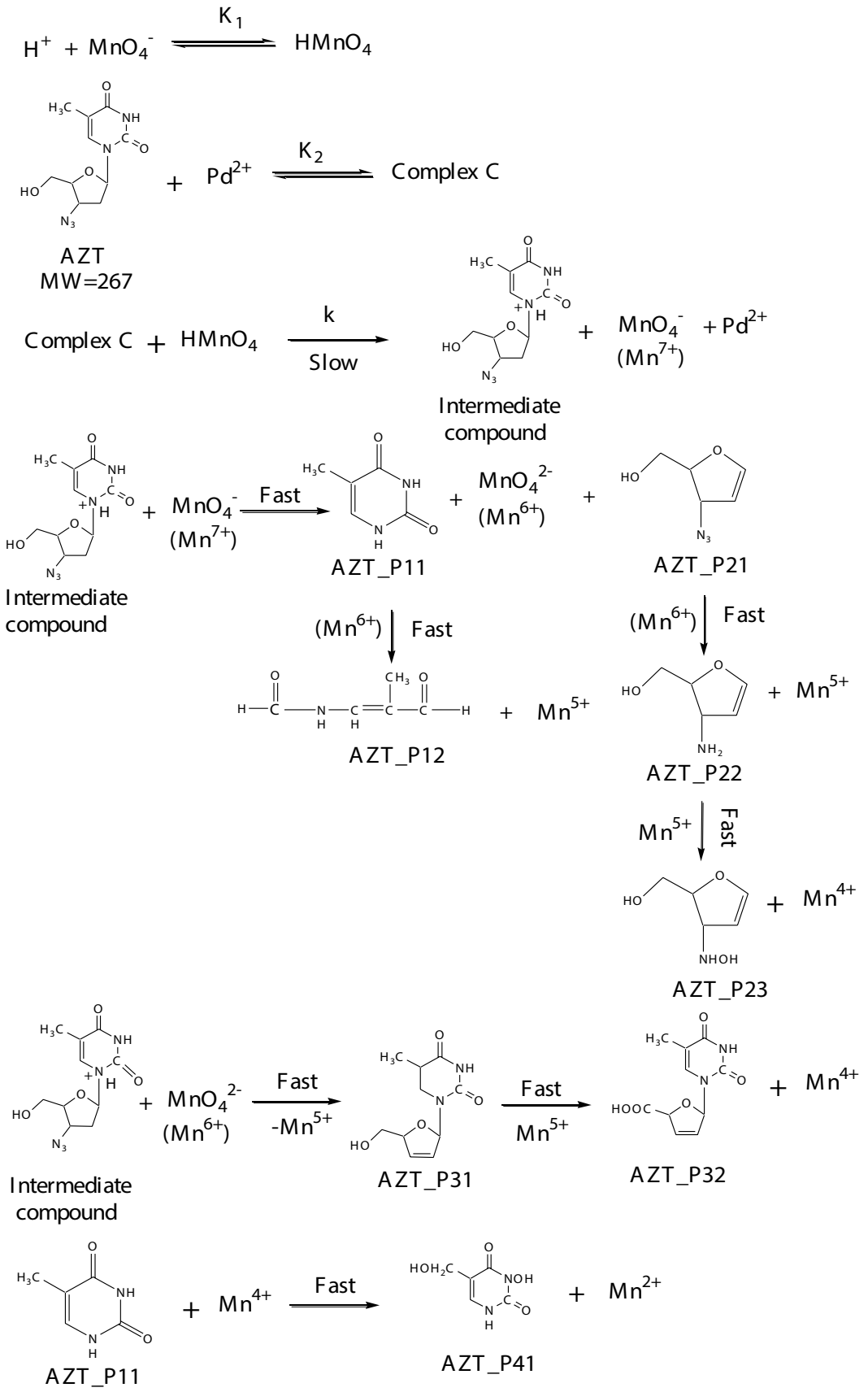

Scheme 1. The proposed Pd^{2+} catalytic mechanism of oxidative degradation of AZT by Mn^{7+} in acidic medium (pH 6.0).

kinetic data that values of rate constants are lower in alkaline medium than in acidic medium which indicates heptavalent manganese is a dominant species in alkaline medium. The chemical equilibrium established can be expressed by Eq. (8) with equilibrium constant (K_1) as follows:

$$H^+ + MnO_4^- \overset{K_1}{\rightleftharpoons} HMnO_4 \quad (8)$$

$$K_1 = \frac{[HMnO_4]}{[H^+][MnO_4^-]} \quad (9)$$

Stoichiometry between AZT and heptavalent manganese was observed 1:1 with unit order dependence on [heptavalent manganese] and [Pd^{2+}] and fractional orders with respect to [AZT] and [H^+] ion. Using kinetic experimental data, a catalytic plausible mechanism projected for the oxidative degradation of AZT by heptavalent manganese in acidic medium includes all the observed orders of [Mn^{7+}], [AZT], [Pd^{2+}], and [H^+]. The different by-products formed were identical in Pd^{2+} catalytic and noncatalytic reactions. HR-MS data show a sodiated molecular ion peak at 290.08 m/z for the standard AZT compound. HR-MS data give eight molecular ion peaks which show that eight number of oxidative degraded products of AZT are formed during Pd^{2+} catalytic oxidative degradation of AZT by heptavalent manganese in acidic medium (pH 6.0). According to Scheme 1 for Pd^{2+}-projected catalytic mechanism, the term K_1 is the equilibrium constant for first equilibrium step established between heptavalent manganese and H^+ ion which forms permanganic acid. $HMnO_4$ is the strongest active species as compared with oxidant heptavalent manganese in acidic medium. K_2 is the equilibrium constant for second equilibrium step, which shows the interaction between the substrate AZT and the potential catalyst Pd^{2+} to form complex C. Then protonated intermediate compound is formed in the next slow step between the complex C and the active species $HMnO_4$. The rate constant for this formation of protonated intermediate compound is k. Then in the next fast steps, this unstable intermediate compound is degraded into various eight by-products. Mn^{7+} species reduced to Mn^{6+} species and breaks the intermediate compound into two oxidative degraded products labelled as AZT_P11 (first degraded product) identified at molecular ion peak 149.02 m/z as stavudine compound and AZT_P21 (second degraded product) identified at observed molecular ion peak 140.90 m/z. Then Mn^{6+} species gets reduced into Mn^{5+} species and breaks the degraded product AZT_P11 further into another oxidative degraded product labelled as AZT_P12 (third degraded product). This AZT_P12 degraded product was identified at molecular ion peak 113.09 m/z formed due to breaking of stavudine compound ring which contains two aldehyde groups (–CHO group). Mn^{6+} also reduces to Mn^{5+} and oxidizes the degraded product AZT_P21 further into another oxidized product labelled as AZT_P22 (fourth degraded product) identified at molecular ion peak 114.05 m/z due to the removal of N_2 and conversion of azide group (N_3) into amino group ($–NH_2$), and Mn^{6+} itself reduces to Mn^{5+}. Mn^{5+} species then reduces to Mn^{4+} and oxidizes the degraded product AZT_P22 further into AZT_P23 (fifth degraded product) identified at observed molecular ion peak 130.90 m/z, and it is formed due to the further oxidation of an amino group ($–NH_2$) to hydroxyl amine (–NHOH) group. Mn^{6+} reduces to Mn^{5+} and oxidizes the protonated AZT intermediate compound to another degraded product labelled as AZT_P31 (sixth degraded product) identified at observed molecular ion peak 224.07 m/z. This AZT_P31 is a thymine compound which is formed by the removal of azide group from the ring of protonated intermediate AZT compound. Further in the next step, Mn^{5+} reduces to Mn^{4+} and oxidizes AZT_P31 to AZT_P32 (seventh degraded product) identified at molecular ion peak 239.91 m/z due to the further oxidation of $–CH_2OH$ group of thymine to carboxylic (–COOH) group. Then Mn^{4+} reduces itself to Mn^{2+} and oxidizes AZT_P11 into another oxidative degraded product labelled as AZT_P41 (eighth degraded product) identified at observed molecular ion peak 181.96 m/z. This oxidative degraded product AZT_P41 is formed due to the oxidation of methyl group ($–CH_3$) into alcohol group ($–CH_2OH$) and –NH group into –NHOH group.

A CARY 50 Bio UV-vis spectrophotometer (Varian BV, The Netherlands) having temperature controller was used to record the UV-vis spectra of AZT (2.0×10^{-4} mol dm^{-3}), the catalyst Pd^{2+} (5×10^{-8} mol dm^{-3}), and a mixture of substrate-catalyst. This UV-vis spectral data give the spectroscopic evidence for the formation of complex between the substrate AZT and the catalyst Pd^{2+} during the Pd^{2+} catalytic oxidative degradation of AZT by heptavalent manganese in acidic medium. By using experimental kinetic data, graphs of [Pd^{2+}]/k_C vs. 1/[AZT] (Fig. 5) and [Pd^{2+}]/k_C vs. 1/[H^+] were plotted and found linear with a positive intercept which confirms the formation of complex between the catalyst Pd^{2+} and the substrate AZT. It was observed from Michaelis-Menton plot that the order with respect to substrate AZT is less than unity, and it confirms the formation of complex between substrate AZT and catalyst Pd^{2+}. The formation of complex between substrate and catalyst was also reported in earlier investigations [10,29] to form degraded products of AZT during water

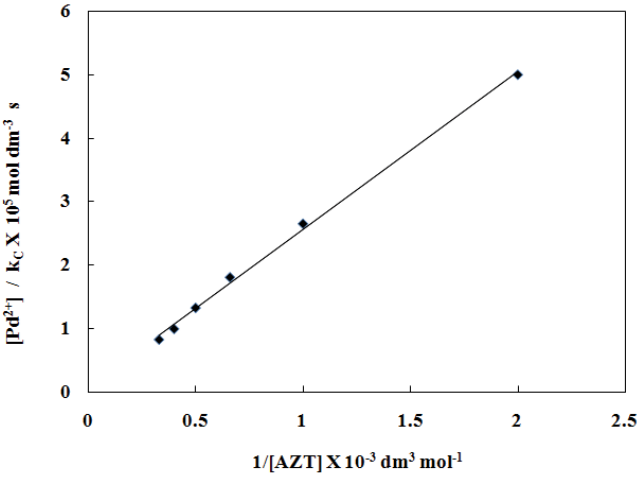

Fig. 5. Plot of [Pd^{2+}]/k_C vs. 1/[AZT] for Pd^{2+} catalytic oxidative degradation of AZT by permanganate in acidic medium at pH 6.0 and temperature 298 K for the verification of rate law Eq. (20). [AZT] = 5×10^{-4} to 3×10^{-3} mol dm^{-3}, [Mn^{7+}] = 1×10^{-4} mol dm^{-3}, [Pd^{2+}] = 5×10^{-8} mol dm^{-3}, [Buffer] = 6×10^{-3} mol dm^{-3}, and ionic strength (I) = 0.02 mol dm^{-3}.

treatment (Fig. S6). Palladium (II) chloride is used as a homogeneous catalyst in many studies. In this study, Palladium (II) chloride is dissolved in suitable quantity of HCl and then in double-distilled water. Palladium (II) chloride exists as $[PdCl_4]^{2-}$ in the presence of chloride ion. $[PdCl_4]^{2-}$ hydrolyzed to $[PdCl_3 (H_2O)]^-$ and forms a complex C with AZT [22,29]. The complex C is then easily protonated in acidic condition and in the presence of catalyst [23]. The proposed structure of complex C formed between AZT and Pd^{2+} is

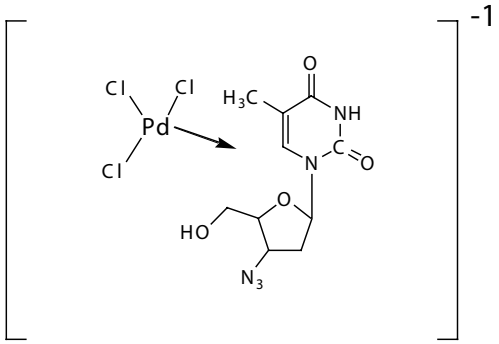

As per the proposed catalytic mechanism (Scheme 1), the rate of the reaction for the slow step by using rate law can be expressed as follows:

$$\text{Rate} = \frac{-d\left[\text{MnO}_4^-\right]}{dt} = k\left[\text{complex } C\right]\left[\text{HMnO}_4\right] \quad (10)$$

From the Eq. (9), we can write an expression for the $[HMnO_4]$ as follows:

$$\left[\text{HMnO}_4\right] = K_1\left[\text{H}^+\right]\left[\text{MnO}_4^-\right] \quad (11)$$

The equilibrium constant K_2 for the formation of complex C can be written as

$$K_2 = \frac{\left[\text{complex C}\right]}{\left[\text{AZT}\right]\left[\text{Pd}^{2+}\right]} \quad (12)$$

$$\left[\text{complex C}\right] = K_2\left[\text{AZT}\right]\left[\text{Pd}^{2+}\right] \quad (13)$$

Putting the values of the complex C and $[HMnO_4]$ in the above Eq. (10), we get

$$\text{Rate} = \frac{-d\left[\text{MnO}_4^-\right]}{dt} = kK_1K_2\left[\text{AZT}\right]_f\left[\text{MnO}_4^-\right]_f\left[\text{Pd}^{2+}\right]_f\left[\text{H}^+\right]_f \quad (14)$$

The term *f* which is used in the above Eq. (14) denotes free concentrations of AZT, MnO_4^-, Pd^{2+}, and H^+. In order to put these values of free concentrations of AZT, MnO_4^-, Pd^{2+}, and H^+, the total concentration of these terms $[AZT]_T$, $[MnO_4^-]_T$, $[Pd^{2+}]_T$, and $[H^+]_T$ should be used as follows:

$$\left[\text{MnO}_4^-\right]_T = \left[\text{MnO}_4^-\right]_f + \left[\text{HMnO}_4\right] + \left[\text{complex C}\right]$$

$$\left[\text{MnO}_4^-\right]_T = \left[\text{MnO}_4^-\right]_f + K_1\left[\text{H}^+\right]\left[\text{MnO}_4^-\right]_f + K_1K_2\left[\text{AZT}\right]\left[\text{H}^+\right]\left[\text{MnO}_4^-\right]_f$$

$$\left[\text{MnO}_4^-\right]_T = \left[\text{MnO}_4^-\right]_f\left\{1 + K_1\left[\text{H}^+\right] + K_1K_2\left[\text{H}^+\right]\left[\text{AZT}\right]\right\}$$

From the above equation, the value of $[MnO_4^-]_f$ can be written as

$$\left[\text{MnO}_4^-\right]_f = \frac{\left[\text{MnO}_4^-\right]_T}{1 + K_1\left[\text{H}^+\right] + K_1K_2\left[\text{H}^+\right]\left[\text{AZT}\right]} \quad (15)$$

The total concentration for H^+ ion can be written as,

$$\left[\text{H}^+\right]_T = \left[\text{H}^+\right]_f + \left[\text{HMnO}_4\right]$$

$$\left[\text{H}^+\right]_T = \left[\text{H}^+\right]_f + K_1\left[\text{H}^+\right]\left[\text{MnO}_4\right]$$

The value of $[H^+]$ ions is very small, and hence, the value of the term K_1 $[H^+]$ $[MnO_4^-]$ is extremely small which can be neglected. Hence, the above equation of $[H^+]_T$ becomes

$$\left[\text{H}^+\right]_T = \left[\text{H}^+\right]_f \quad (16)$$

Similarly, the total concentration of AZT can be written as

$$\left[\text{AZT}\right]_T = \left[\text{AZT}\right]_f \quad (17)$$

The total concentration of the catalyst Pd^{2+} can be expressed as

$$\left[\text{Pd}^{2+}\right]_T = \left[\text{Pd}^{2+}\right]_f + \left[\text{complex C}\right]$$

$$\left[\text{Pd}^{2+}\right]_T = \left[\text{Pd}^{2+}\right]_f + K_2\left[\text{AZT}\right]\left[\text{Pd}^{2+}\right]_f$$

$$\left[\text{Pd}^{2+}\right]_T = \left[\text{Pd}^{2+}\right]_f + \left\{1 + K_2\left[\text{AZT}\right]\right\}$$

$$\left[\text{Pd}^{2+}\right]_f = \frac{\left[\text{Pd}^{2+}\right]_T}{1 + K_2\left[\text{AZT}\right]}$$

In this above equation, the product of concentration of AZT and K_2 is very small, and hence, it can be ignored. Then, the above equation of the free concentration of catalyst Pd^{2+} becomes as

$$\left[\text{Pd}^{2+}\right]_f = \left[\text{Pd}^{2+}\right]_T \quad (18)$$

Putting the values of $[MnO_4^-]_f$, $[AZT]_f$, $[H^+]_f$, and $[Pd^{2+}]_f$ with omitting the subscripts in the above mentioned Eq. (15), we get a new equation as

$$\text{Rate} = \frac{-d\left[\text{MnO}_4^-\right]}{dt} = \frac{kK_1K_2\left[\text{MnO}_4^-\right]\left[\text{AZT}\right]\left[\text{H}^+\right]\left[\text{Pd}^{2+}\right]}{1+K_1\left[H^+\right]+K_1K_2\left[\text{H}^+\right]\left[\text{AZT}\right]} \quad (19)$$

$$\frac{\text{Rate}}{\left[\text{MnO}_4^-\right]} = k_C = k_O - k_U = \frac{kK_1K_2\left[\text{MnO}_4^-\right]\left[\text{AZT}\right]\left[\text{H}^+\right]\left[\text{Pd}^{2+}\right]}{1+K_1\left[\text{H}^+\right]+K_1K_2\left[\text{H}^+\right]\left[\text{AZT}\right]} \quad (20)$$

The above mentioned rate law Eq. (20) can be rearranged in the following form:

$$\frac{\left[\text{Pd}^{2+}\right]}{k_C} = \frac{1}{kK_1K_2\left[\text{AZT}\right]\left[\text{H}^+\right]} + \frac{1}{kK_2\left[\text{AZT}\right]} + \frac{1}{k} \quad (21)$$

From Eq. (21), if the graphs of $[Pd^{2+}]/k_C$ vs. 1/[AZT] and $[Pd^{2+}]/k_C$ vs. 1/[H^+] are plotted, then it should be linear with a positive intercept. This was observed in Michaelis-Menton plot, which confirms the formation of complex between the catalyst Pd^{2+} and substrate AZT. The slopes and intercept of these plots are used to calculate the values of k, K_1, and K_2. The obtained values of k, K_1, and K_2 from slopes and intercepts of these plots are 4.93×10^{-2} dm^3 mol^{-1} s^{-1}, 39 dm^3 mol^{-1}, and 5.375×10^3 dm^3 mol^{-1}, respectively, at 298 K for the Pd^{2+}-catalyzed reaction. The value of K_1 for the first equilibrium step between MnO_4^- ion and $HMnO_4$ is in good agreement with the earlier investigations in the literature [33]. Using these values of constants, the rate constants were determined under different experimental conditions. These rate constant values were compared with the experimental values of k_C and found in good agreement with each other. This gives the support to the projected Pd^{2+} catalytic mechanism for oxidative degradation of AZT by heptavalent manganese in acidic medium.

The values of activation energy E_a for uncatalyzed and Pd^{2+}-catalyzed reactions were found to be 45.22 ± 2.02 and 40.60 ± 2.00 kJ mol^{-1}, respectively, from the Arrhenius plots of log k vs. 1/T. The values of enthalpy of activation ($\Delta H^{\neq}$), entropy of activation ($\Delta S^{\neq}$), and Gibbs free energy of activation ($\Delta G^{\neq}$) were found to be 42.80 ± 2.00 kJ mol^{-1}, −135.33 ± 14.20 Jk^{-1} mol^{-1}, and 82.09 ± 7.40 kJ mol^{-1}, respectively, for the slow step of uncatalyzed reaction. The values of $\Delta H^{\neq}$, $\Delta S^{\neq}$, and $\Delta G^{\neq}$ were found to be 38.18 ± 1.50 kJ mol^{-1}, −142.01 ± 13.20 Jk^{-1} mol^{-1}, and 80.64 ± 6.30 kJ mol^{-1}, respectively, for Pd^{2+}-catalyzed reaction. The value of E_a is found to be higher in noncatalytic reaction than Pd^{2+} catalytic reaction, which shows that catalyst Pd^{2+} lowers the energy barrier and modifies the path of oxidative degradation of AZT by heptavalent manganese in acidic medium (pH 6.0) for the catalytic reaction.

The value of $\Delta S^{\neq}$ is found to be negative as shown in Table 3. The higher negative value of $\Delta S^{\neq}$ indicates the formation of more activated complex between the substrate AZT and catalyst Pd^{2+}. The negative value of entropy of activation shows that activated complex is more ordered as compared with reactants [10,34–37]. The values of $\Delta G^{\neq}$ for noncatalytic and Pd^{2+} catalytic oxidative degradation of AZT by heptavalent manganese in acidic medium (pH 6.0) were calculated by using values of $\Delta H^{\neq}$ and $\Delta S^{\neq}$. The values of $\Delta G^{\neq}$ and $\Delta H^{\neq}$ indicate that the transition state is more solvated in Pd^{2+} catalytic reaction as compared with noncatalytic reaction. The calculated values of E_a, $\Delta G^{\neq}$, and $\Delta S^{\neq}$ indicate that catalyst Pd^{2+} forms an activated complex C as compared with other catalyst. The projected Pd^{2+} catalytic mechanism is in good agreement with the observed rate law for the Pd^{2+}-catalyzed oxidative degradation of AZT by heptavalent manganese in acidic medium (pH 6.0) [38]. The values of activation parameters elucidate that catalyst Pd^{2+} accelerates the rate of oxidative degradation reaction. Hence, Pd^{2+} plays a very vital role in the removal of AZT by heptavalent manganese in acidic medium (pH 6.0) due to its effective catalytic activity. The use of Pd^{2+} catalyst in this oxidative degradation of AZT by heptavalent manganese in acidic medium enhances the reducing property of AZT in catalyzed reaction than uncatalyzed reaction due to the formation of a complex C between AZT and the catalyst Pd^{2+}. It indicates that Pd^{2+} provides a new lower path for the reactants to form oxidative degraded products. It shows that the catalyst Pd^{2+} permits the reactants to a great extent to obtain sufficient energy to pass through the transition state and form eight degraded products [10,23]. The kinetic data regarding the effect of variation in ionic strength (I) confirm that the influence of ionic strength (I) is insignificant in noncatalytic and Pd^{2+} catalytic oxidative degradation of AZT by heptavalent manganese in acidic medium. It did not affect the values of the rate constants of noncatalytic and Pd^{2+} catalytic oxidative degradation reactions. The negligible effect of ionic strength (I) on the values of rate constants proves that the noncatalytic and catalytic oxidative degradation reactions are between neutral and charged species or two neutral species [39], while in the oxidation of *L*-proline, the reaction is between two negatively charged species due to the intervention of free radicals [38]. The graphs of log k_{obs} vs. 1/D were plotted for noncatalytic and Pd^{2+} catalytic reactions. These plots are straight lines with negative slopes for both reactions. The variation in solvent polarity confirms that noncatalytic or Pd^{2+} catalytic oxidative degradation of AZT by heptavalent manganese in acidic medium is between two dipoles [40].

Table 3
Activation parameters from the influence of variation in temperature for uncatalyzed and Pd^{2+}-catalyzed oxidative degradation of AZT by heptavalent manganese at pH 6.0. $[Mn^{7+}] = 1 \times 10^{-4}$ mol dm^{-3}, [AZT] = 5×10^{-4} to 3×10^{-3} mol dm^{-3}, $[Pd^{2+}] = 5 \times 10^{-8}$ mol dm^{-3},[Buffer] = 6×10^{-3} mol dm^{-3}, and ionic strength (I) = 0.02 mol dm^{-3}

Activation parameters (kJ mol–1)	Values for uncatalyzed reaction	Values for Pd^{2+}-catalyzed reaction
Ea	45.22 ± 2.02	40.60 ± 2.00
$\Delta H^{\neq}$	42.80 ± 2.00	38.18 ± 1.50
$\Delta S^{\neq}$	−135.33 ± 14.20	−142.01 ± 13.20
$\Delta G^{\neq}$	82.09 ± 7.40	80.64 ± 6.30

The concentration of catalyst Pd^{2+} used for oxidation of AZT by heptavalent manganese at pH 6.0 is an extremely small (10^{-8} mol dm^{-3}) as compared with the concentration of Pd^{2+} (10^{-5} mol dm^{-3}) used for the oxidation of *L*-proline by heptavalent manganese in alkaline medium. Hence, the catalyst Pd^{2+} is found to be very effective for the oxidation of AZT by heptavalent manganese at environmentally relevant pH than *L*-proline by heptavalent manganese in alkaline medium. The oxidation of AZT is carried out at acidic pH 6.0, which is environmentally relevant pH and will not have any adverse impacts on human health and animals. On the other hand, the oxidation of *L*-proline was performed at alkaline pH using strong alkali NaOH [38], which is not environmentally relevant medium for the treatment of water. The oxidation of *L*-proline using strong alkali NaOH will have adverse impacts on human health and animals. The polymerization study reveals that there was no intervention of free radicals in the present study while there was no intervention of free radicals in *L*-proline system.

4. Conclusion

(1) The rate of the removal of AZT was found faster in Pd^{2+}-catalyzed oxidative degradation of AZT with heptavalent manganese in acidic medium than uncatalyzed reaction. (2) $HMnO_4$ and catalyst Pd^{2+} are found to be active species in acidic medium. This concludes that pH of the medium plays an important role in this Pd^{2+} catalytic reaction. (3) The overall order explained here is reliable with oxidative degraded products and mechanistic and kinetic studies. (4) The calculated values of activation energies conclude that the Pd^{2+} provides a lower path for the formation of oxidative degraded products of AZT. (5) The negligible effect of ionic strength (*I*) on the values of rate constants concludes that the noncatalytic and catalytic oxidative degradation reactions are between neutral and charged species or two neutral species. (6) The effect of variation in solvent polarity concludes that the noncatalytic or Pd^{2+} catalytic oxidative degradation of AZT by heptavalent manganese in acidic medium is between two dipoles. (7) The projected Pd^{2+} catalytic mechanism is in good agreement with the observed rate law. This present study concludes that catalyst Pd^{2+} is a very efficient and potential catalyst for the removal of antiretroviral drug AZT at environmentally relevant pH (6.0).

References

[1] R. Braund, B. Peake, A. Tong, Disposal practices for unused medications around the world, Environ. Int., 37 (2011) 292–298.

[2] V.S. Bhamare, R.M. Kulkarni, B. Santhakumari, Uncatalysed kinetic and mechanistic investigation of oxidative degradation of antibacterial drug linezolid by heptavalent manganese at environmentally relevant pH, Int. J. Adv. Res. Sci. Eng. Technol., 7 (2018) 706–721.

[3] A.A.P. Khan, A.M. Asiri, N. Azum, M.A. Rub, A. Khan, A.O. Al-Youbi, Kinetics and mechanistic investigation of decarboxylation for the oxidation of levofloxacin by Chloroamine-T in acidic medium, Ind. Eng. Chem. Res., 51 (2012) 4819–4824.

[4] M.W. Lam, C.J. Young, R.A. Brain, D.J. Johnson, M.A. Hanson, C.J. Wilson, S.M. Richards, K.R. Solomon, S.A. Mabury, Aquatic persistence of eight pharmaceuticals in a microcosm study, Environ. Toxicol. Chem., 23 (2004) 1431–1440.

[5] G. Stiver, The treatment of influenza with antiviral drugs, CMAJ., 168 (2003) 49–56.

[6] P. Kumar, P.S.K. Kumar, R.M. Kulkarni, Fate of zidovudine through water treatment with chlorine: a kinetic study, Int. Res. J. Environ. Sci., 3 (2014) 50–55.

[7] M.A. Fischl, D.D. Richman, M.H. Grieco, M.S. Gottlieb, P.A. Volberding, O.L. Laskin, J.E. Leedom, J.E. Groopman, D. Mildvan, D. Mildran, R.T. Schooley, The efficacy of azidothymidine (AZT) in the treatment of patients with AIDS and AIDS related complex A double-blind placebo control trial, N. Engl. J. Med., 317 (1987) 185–191.

[8] A.R. Gennaro, Remington: The Science and Practice of Pharmacy, Mack Publishing Company, Easton, PA, 1995.

[9] S. Budavari, The Merck Index, Merck & Co, White House Station, N.J., U.S.A, 1996.

[10] R.M. Kulkarni, M.S. Hanagadakar, R.S. Malladi, B. Santhakumari, S.T. Nandibewoor, Oxidation of linezolid by permanganate in acidic medium: Pd (II) catalysis, kinetics and pathways, Prog. React. Kinet. Mech., 41 (2016) 245–257.

[11] T. Lin, S. Pan, W. Chen, C. Yu, Effect of potassium permanganate pre-oxidation on fouling and pore size of ultra filtration membrane for drinking water treatment, Desal. Wat. Treat., 50 (2012) 254–263.

[12] R.H. Waldemer, P.G. Tratnyek, Kinetics of contaminant degradation by permanganate, Environ. Sci. Technol., 40 (2006) 1055–1061.

[13] R.M. Kulkarni, M.S. Hanagadakar, R.S. Malladi, H.S. Biswal, E.M. Cuerda-Correa, Experimental and theoretical studies on the oxidation of lomefloxacin by alkaline permanganate, Desal. Wat. Treat., 57 (2016) 10826–10838.

[14] R.M. Kulkarni, M.S. Hanagadakar, R.S. Malladi, N.P. Shetti, Ag(I)-Catalyzed chlorination of linezolid during water treatment: kinetics and mechanism, Int. J. Chem. Kinet., 50 (2018) 495–506.

[15] R.M. Kulkarni, D.C. Bilehal, S.T. Nandibewoor, Deamination and decarboxylation in the chromium(III)-catalysed oxidation of L-valine by alkaline permanganate and analysis of chromium (III) in microscopic amounts by a kinetic method, Transition Met. Chem., 28 (2003) 199–208.

[16] D.C. Bilehal, R.M. Kulkarni, S.T. Nandibewoor, Comparative study of the chromium (III) catalysed of L-leucine and L-isoleucine by alkaline permanganate, J. Mol. Catal. A: Chem., 232 (2005) 21–28.

[17] R.M. Kulkarni, V.S. Bhamare, B. Santhakumari, Mechanistic and spectroscopic investigations of Ru^{3+}-catalyzed oxidative degradation of azidothymidine by heptavalent manganese at environmentally relevant pH, Desal. Wat. Treat., 57 (2016) 28349–28362.

[18] K.A. Thabaj, S.A. Chimatadar, S.T. Nandibewoor, Mechanistic study of oxidation of palladium (II) by cerium (IV) in aqueous acid, Transition Met. Chem., 31 (2006) 186–193.

[19] S.A. Chimatadar, S.B. Koujalagi, S.T. Nandibewoor, Kinetics and mechanism of palladium (II) catalysed chromium (VI) oxidation of mercury (I) in aqueous sulphuric acid, Transition Met. Chem., 26 (2001) 662–667.

[20] A.K. Singh, R. Negi, B. Jain, Y. Katre, S.P. Singh, V.K. Sharma, Pd (II) catalysed oxidative degradation of paracetamol by chloramine -T in acidic and alkaline media, Ind. Eng. Chem. Res.,50 (2011) 8407–8419.

[21] S.P. Singh, A.K. Singh, B. Singh, Mechanistic study of palladium (II) catalysed oxidation of crotonic acid by periodate in aqueous perchloric acid medium, J. Mol. Catal. A: Chem., 266 (2007) 226–232.

[22] A.K. Singh, J. Bhawana, R. Negi, Y. Katre, S.P. Singh, Oxidation of valine by N-bromophthalimide in presence of chloro-complex of Pd(II) as homogenous catalyst: a kinetic and mechanistic study, Open Catal. J., 2 (2009) 12–20.

[23] M.K. Ghosh, S.K. Rajput, Kinetics and mechanism of Palladium (II) catalyzed oxidation of D-(+) galactose by cerium (IV) in aqueous acidic medium, Am. Chem. Sci. J., 4 (2014) 384–400.

[24] G.H. Jeffery, J. Bassett, J. Mendham, R.C. Denny, Vogel's Textbook of Quantitative Chemical Analysis, ELBS, Longman, Essex, UK, 1996.

[25] L.I. Simandi, M. Jaky, C.R. Savage, Z.A. Schelly, Kinetics and mechanism of the permanganate ion oxidation of sulfite in alkaline solutions. The nature of short-lived intermediates, J. Am. Chem. Soc., 107 (1985) 4220–4224.
[26] R.M. Kulkarni, V.S. Bhamare, B. Santhakumari, Oxidative transformation of antiretroviral drug zidovudine during water treatment with permanganate: reaction kinetics and pathways, Desal. Wat. Treat., 57 (2016) 24999–25010.
[27] G.C. Hiremath, R.M. Kulkarni, S.T. Nandibewoor, Kinetics of oxidative degradation and deamination of atenolol by aqueous alkaline permanganate, Indian J. Chem. Sect. A, 44 (2005) 245–250.
[28] D.G. Richard, Introduction to Physical Organic Chemistry, Addison Wesley Publishing Company, London, 1970.
[29] J.C. Abbar, S.D. Lamani, S.T. Nandibewoor, Ruthenium (III) catalysed oxidative degradation of amitriptyline-A tricyclic antidepressant drug by permanganate in aqueous acidic medium, J. Solution Chem., 40 (2011) 502–520.
[30] S. Bhattacharya, P. Banerjee, Kinetic studies on the electron transfer between azide and nickel (IV) oxime imine complexes in aqueous solution, Bull. Chem. Soc. Jpn., 69 (1996) 3475–3482.
[31] E.A. Moelwyn-Hughes, Kinetics of Reaction in Solutions, Oxford University Press, London, 1947.
[32] P.L. Timmanagoudar, G.A. Hiremath, S.T. Nandibewoor, Permanganate oxidation of thallium (I) in sulphuric acid: A kinetic study by stopped flow technique, Pol. J. Chem., 70 (1996) 1459–1467.
[33] M.B. Patgar, M.D. Meti, S.T. Nandibewoor, S.A. Chimatadar, Kinetics and mechanism of oxidation of an antiarrhythmic drug procainamide hydrochloride by Mn (VII) in aqueous sulphuric acid medium: a stopped flow technique, Int. J. Pharm. Pharm. Sci., 6 (2014) 583–588.
[34] K.S. Rangappa, N. Anitha, N.M. Madegouda, Mechanistic investigation of the oxidation of substituted phenethyl alcohols by manganese (III) sulphate catalysed by ruthenium (III) in acid solution, Synth. React. Inorg. Met.-Org. Chem., 31 (2001) 1499–1518.
[35] Z.D. Bugarcic, S.T. Nandibewoor, M.S.A. Hamza, F. Heinemann, R. van Eldik, Kinetics and mechanism of the reactions of Pd (II) complexes with azoles and diazines crystal structure of [Pd (bpma) (H_2O)] (ClO_4)$_2$. 2H_2O, Dalton Trans., 24 (2006) 2984–2990.
[36] A.A.P. Khan, A. Khan, A.M. Asiri, N. Azum, M.A. Rub, Micro concentrations of Ru (III) used as homogenous catalyst in the oxidation of levothyroxine by N-bromosuccinimide and the mechanistic pathway, J. Taiwan Inst. Chem. Eng., 45 (2014) 127–133.
[37] A.M. Asiri, A.A.P. Khan, A. Khan, Spectroscopic investigation on kinetics and mechanistic aspects to electron-transfer process into quinolinium dichromate oxidation of a high blood pressure drug captopril in acidic medium, J. Mol. Liq., 203 (2015) 1–6.
[38] V.C. Seregar, C.V. Hiremath, S.T. Nandibewoor, Palladium (II) Catalysed oxidation of l-proline by heptavalent manganese in aqueous alkaline medium: A free radical intervention and decarboxylation, Transition Met. Chem., 31 (2006) 541–548.
[39] K.J. Laidler, Chemical Kinetics, Pearson Education Ltd., Indian Branch, Delhi, India, 2004.
[40] E.S. Amis, Solvent Effects on Reaction Rates and Mechanisms, Academic Press, New York, 1966.

Supplementary Information

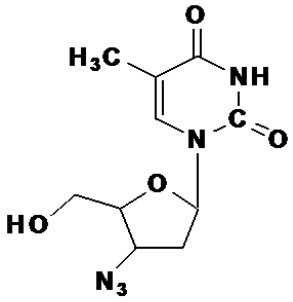

Fig. S1. Structure of azidothymidine (AZT).

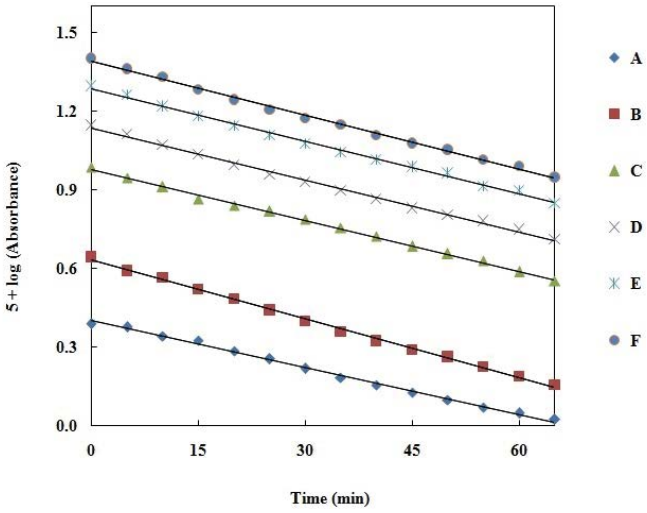

Fig. S2. Pseudo-first-order plots of the oxidative degradation of AZT by heptavalent manganese in acidic medium at pH 6.0 and temperature 298 K. [Mn^{7+}] = 1 × 10^{-4} mol dm^{-3}: (a) 0.25, (b) 0.50, (c) 1.0, (d) 1.5, (e) 2.0, and (f) 2.5, [AZT] = 1 × 10^{-3} mol dm^{-3}, [Buffer] = 6 × 10^{-3} mol dm^{-3}, and ionic strength (I) = 0.02 mol dm^{-3}.

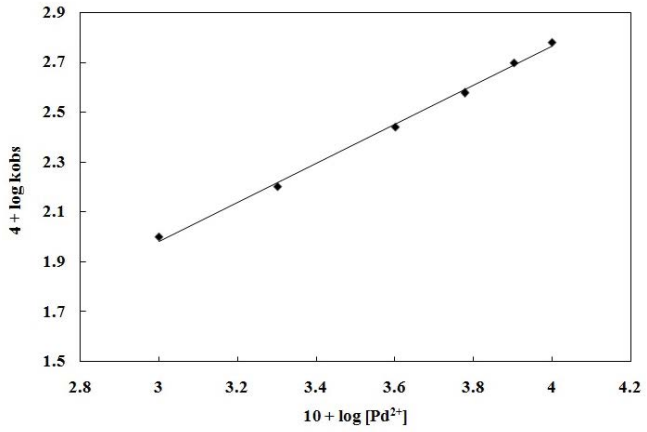

Fig. S3. Influence of variation in concentration of Pd^{2+} on oxidative degradation of AZT by heptavalent manganese in acidic medium at pH 6.0 and temperature 298 K. [Pd^{2+}] = 1.0 × 10^{-8} mol dm^{-3} to 1.0 × 10^{-7} mol dm^{-3}, [Mn^{7+}] = 1 × 10^{-4} mol dm^{-3}, [AZT] = 1 × 10^{-3} mol dm^{-3}, [Buffer] = 6 × 10^{-3} mol dm^{-3}, and ionic strength (I) = 0.02 mol dm^{-3}.

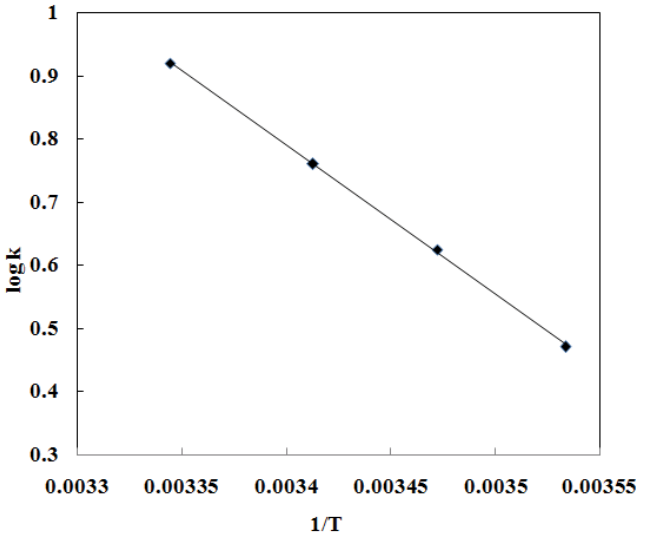

Fig. S4. Arrhenius plot of log k vs. $1/T$ for four different temperatures 283, 288, 296, and 299 K by varying [AZT] from 5×10^{-4} to 3×10^{-3} mol dm^{-3}, while freezing other experimental conditions such as [Mn^{7+}] = 1×10^{-4} mol dm^{-3}, [Buffer] = 6×10^{-3} mol dm^{-3}, and ionic strength (I) = 0.02 mol dm^{-3} for uncatalyzed oxidative degradation of AZT by heptavalent manganese in acidic medium (pH 6.0).

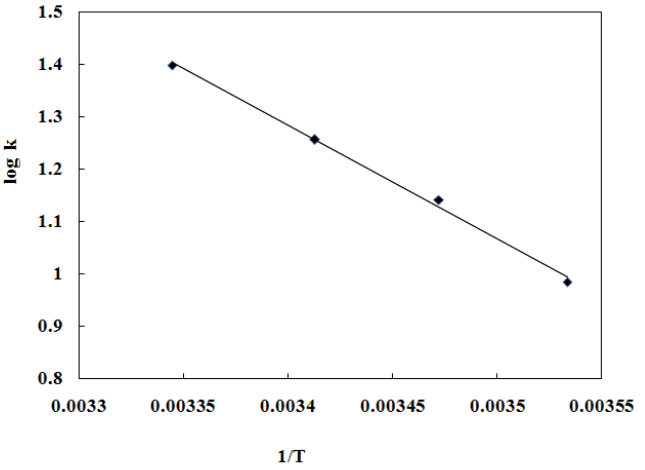

Fig. S5. Arrhenius plot of log k vs. $1/T$ for four different temperatures 283, 288, 296, and 299 K by varying [AZT] from 5×10^{-4} to 3×10^{-3} mol dm^{-3}, while freezing other experimental conditions such as [Mn^{7+}] = 1×10^{-4} mol dm^{-3}, [Pd^{2+}] = 5×10^{-8} mol dm^{-3}, [Buffer] = 6×10^{-3} mol dm^{-3}, and ionic strength (I) = 0.02 mol dm^{-3}.

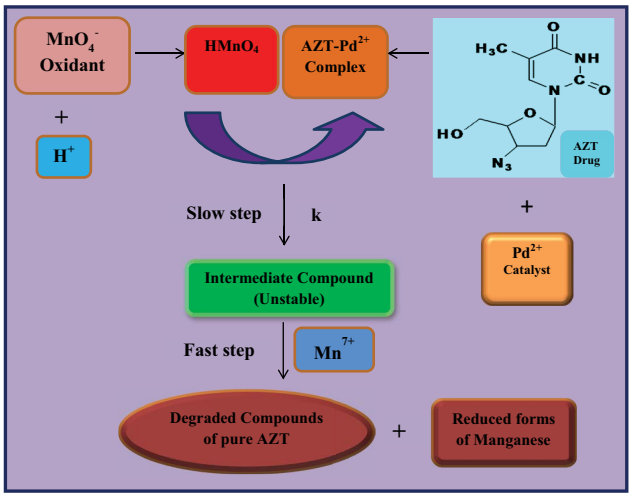

Fig. S6. The formation of complex between substrate and catalyst to form degraded compounds of AZT and reduced forms of manganese during water treatment process.